

ORIGINAL ARTICLE

# Piceamycin and its *N*-acetylcysteine adduct is produced by *Streptomyces* sp. GB 4-2\*

Dirk Schulz<sup>1,6</sup>, Jonny Nachtigall<sup>2,6</sup>, Julia Riedlinger<sup>1</sup>, Kathrin Schneider<sup>2</sup>, Karl Poralla<sup>1</sup>, Johannes F Imhoff<sup>3</sup>, Winfried Beil<sup>4</sup>, Graeme Nicholson<sup>5</sup>, Hans-Peter Fiedler<sup>1</sup> and Roderich D Süssmuth<sup>2</sup>

**Piceamycin, a new macrolactam polyketide antibiotic, was detected by HPLC-diode array screening in extracts of *Streptomyces* sp. GB 4-2, which was isolated from the mycorrhizosphere of Norway spruce. The structure of piceamycin was determined by mass spectrometry and NMR experiments. It showed inhibitory activity against Gram-positive bacteria, selected human tumor cell lines and protein tyrosine phosphatase 1B.**

*The Journal of Antibiotics* (2009) 62, 513–518; doi:10.1038/ja.2009.64; published online 17 July 2009

**Keywords:** macrolactam antibiotic; polyketide; protein tyrosine phosphatase 1B inhibitor; *Streptomyces*; structural elucidation

## INTRODUCTION

The rhizosphere is a highly complex and evidently balanced community of symbiotic and parasitic organisms composed by the coexistence of plants, mycorrhiza-forming soil fungi and mycorrhiza-promoting bacteria, on the one hand, and phytopathogenic fungi and bacteria on the other.<sup>2</sup> On account of the attack and defense mechanisms within this community, a huge variety of signaling factors, growth-promoting metabolites, antifungals and phytotoxins produced by the various partners of this interaction have been reported.<sup>3,4</sup> Recently, we described the mycorrhiza growth-promoting factor, auxofuran, which was produced by the mycorrhiza helper bacterium, *Streptomyces* sp. AcH 505, isolated from the mycorrhizosphere of Norway spruce.<sup>5,6</sup> In addition, the same streptomycete produced two antifungal naphthoquinone antibiotics, WS-5995 B and C, which inhibited the growth of the spruce-pathogenic fungus, *Heterobasidion annosum*.

*Streptomyces* sp. GB 4-2 was isolated from the mycorrhizosphere of Norway spruce (*Picea abies*). In contrast to *Streptomyces* sp. AcH 505, strain GB 4-2 does not act as a mycorrhiza helper bacterium but promotes the growth of the phytopathogenic fungus, *Heterobasidion abietinum* and induces in parallel plant defense responses. Host responses indicated that strain GB 4-2 induced both local and systemic defense responses in Norway spruce.<sup>7</sup> Furthermore, strain GB 4-2 was found to give a response against the attack of *Heterobasidion* toward the host plant by a two-step enzymatic detoxification of the fungal phytotoxin fomannoxin, which will be reported in a forthcoming publication.

In this report, we describe the fermentation, isolation, structural elucidation and biological activity of piceamycin (1), a novel macrocyclic

lactam antibiotic, and its *N*-acetylcysteine adduct (2) produced by the strain, GB 4-2. The structures of 1 and 2 are shown in Figure 1. Piceamycin (1) shows remarkable inhibitory activities against Gram-positive bacteria, human tumor cell lines and human recombinant protein tyrosine phosphatase 1B. The function of 1 within the interaction between the producing strain, Norway spruce, and the parasitic fungus, *Heterobasidion*, is not yet understood, because the compound does not show inhibitory effects against *Heterobasidion* and neither does it induce local and systemic defense response in Norway spruce.

## RESULTS

### Taxonomy of the producing strain

The morphological and chemical properties of strain GB 4-2 designated the strain as belonging to the genus *Streptomyces*.<sup>8,9</sup> The strain divided on agar plates into a grey-sporulating wild-type and a yellow-orange colored mutant with sparsely developed white aerial mycelium. In submerged cultures, only the yellow-orange mutant was observed. The peptidoglycan was rich in LL-diaminopimelic acid and hexa- and octahydrogenated menaquinones with nine isoprene units were the predominant isoprenologs. Partial sequencing of the 16S rRNA gene of strain GB 4-2 was described by Lehr *et al.*<sup>7</sup> and confirmed its taxonomic classification to the genus *Streptomyces*.

### Screening, fermentation and isolation

*Streptomyces* isolated from the rhizosphere of various plants were grown in submerged culture in different complex media, and extracts were prepared from mycelia and culture filtrates at various fermentation

<sup>1</sup>Mikrobiologisches Institut, Universität Tübingen, Tübingen, Germany; <sup>2</sup>Institut für Chemie, Technische Universität Berlin, Berlin, Germany; <sup>3</sup>Kieler Wirkstoffzentrum KiWiZ am Institut für Meeresswissenschaften IFM-GEOMAR, Kiel, Germany; <sup>4</sup>Institut für Pharmakologie, Medizinische Hochschule Hannover, Hannover, Germany and <sup>5</sup>Institut für Organische Chemie, Universität Tübingen, Tübingen, Germany

<sup>6</sup>These authors contributed equally to this work.

Correspondence: Professor H-P Fiedler, Mikrobiologisches Institut, Auf der Morgenstelle 28, Universität Tübingen, 72076 Tübingen, Germany.

E-mail: hans-peter.fiedler@uni-tuebingen.de or

Professor RD Süssmuth, Institut für Chemie, Technische Universität Berlin, Straße des 17. Juni 124, 10623 Berlin, Germany.

E-mail: suessmuth@chem.tu-berlin.de

\*Art. no. 50 in 'Biosynthetic Capacities of Actinomycetes'. Art. no. 49: see Hohmann *et al.*<sup>1</sup>

Received 9 April 2009; revised 25 June 2009; accepted 29 June 2009; published online 17 July 2009

times. The extracts were screened by HPLC-diode array monitoring in combination with our in-house developed HPLC-UV-Vis database<sup>10</sup> to detect novel secondary metabolites. Strain GB 4-2 gained our interest because of the presence of two peaks in the culture filtrate extract at retention times of 8.2 and 10.1 min, as shown in Figure 2, having characteristic UV-visible spectra that differed from those of 867 reference compounds stored in our database.

During a 10-l fermentation strain GB 4-2 began production of **1** after 48 h and reached a maximal yield of  $170 \text{ mg l}^{-1}$  at 96 h of incubation. **2** was produced simultaneously with **1**, though in a reduced amount. **1** was isolated from the culture filtrate by extraction with ethyl acetate and purified by chromatography on a diol-modified silica gel column followed by subsequent chromatography on Sephadex LH-20 and Toyopearl HW-40 columns. Pure **1** was obtained by preparative reversed-phase (RP)-HPLC as an orange powder.

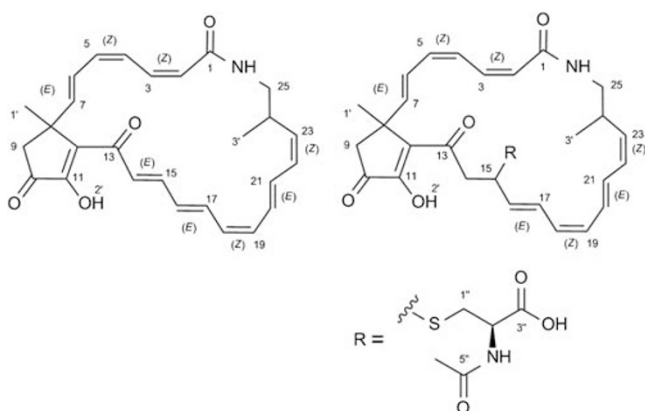


**Figure 1** Structures of piceamycin (**1**) and its N-acetylcysteine adduct (**2**).

**2** was isolated from the culture filtrate by separation on an Amberlite XAD-16 column and was purified by subsequent chromatography on Sephadex LH-20 and Toyopearl HW-40S columns. Pure **2** was obtained by preparative RP-HPLC as pale-yellow powder.

### Structural elucidation

The physico-chemical properties of **1** and **2** are summarized in Table 1. <sup>13</sup>C and <sup>1</sup>H NMR data of **1** and **2** are summarized in Tables 2 and 3, respectively. The molecular masses of **1** and **2** were determined by high-resolution electrospray ionization fourier transform ion cyclotron resonance (ESI-FR-ICR) mass spectrometry, which gave a monoisotopic signal at 432.21697 a.m.u. for **1** and a mass of 595.24699 a.m.u. for **2**, corresponding to  $[\text{C}_{27}\text{H}_{29}\text{NO}_4]^+$  (theoretical: 432.21693 a.m.u. for  $[\text{M}+\text{H}]^+$ ,  $\Delta=0.09$  p.p.m.) for **1** and  $[\text{C}_{32}\text{H}_{39}\text{N}_2\text{O}_7\text{S}]^+$  (theoretical: 595.24725 a.m.u.,  $\Delta=0.44$  p.p.m.) for **2**.

The detailed analyses of COSY (correlated spectroscopy), heteronuclear single quantum coherence (HSQC) and heteronuclear multiple bond coherence (HMBC) NMR spectra enabled the assignment of all proton and carbon NMR signals as shown in Figures 3 and 4. The <sup>1</sup>H, <sup>13</sup>C and HSQC NMR data of **1** revealed the presence of 21 sp<sup>2</sup>-hybridized carbons and one aliphatic methine carbon, two

**Table 1** Physico-chemical properties of **1** and **2**

	<b>1</b>	<b>2</b>
Appearance	Orange powder	Pale-yellow powder
FT-ICR-MS	432.21697 measured (M+H) <sup>+</sup> 432.21693 theoretical $\Delta=0.09$ p.p.m.	595.24699 measured (M+H) <sup>+</sup> 595.24725 theoretical $\Delta=0.44$ p.p.m.
Molecular formula	C <sub>27</sub> H <sub>29</sub> NO <sub>4</sub>	C <sub>32</sub> H <sub>38</sub> N <sub>2</sub> O <sub>7</sub> S
UV $\lambda_{\text{max}}$ (MeOH)	295, 410	295, 330 (sh)

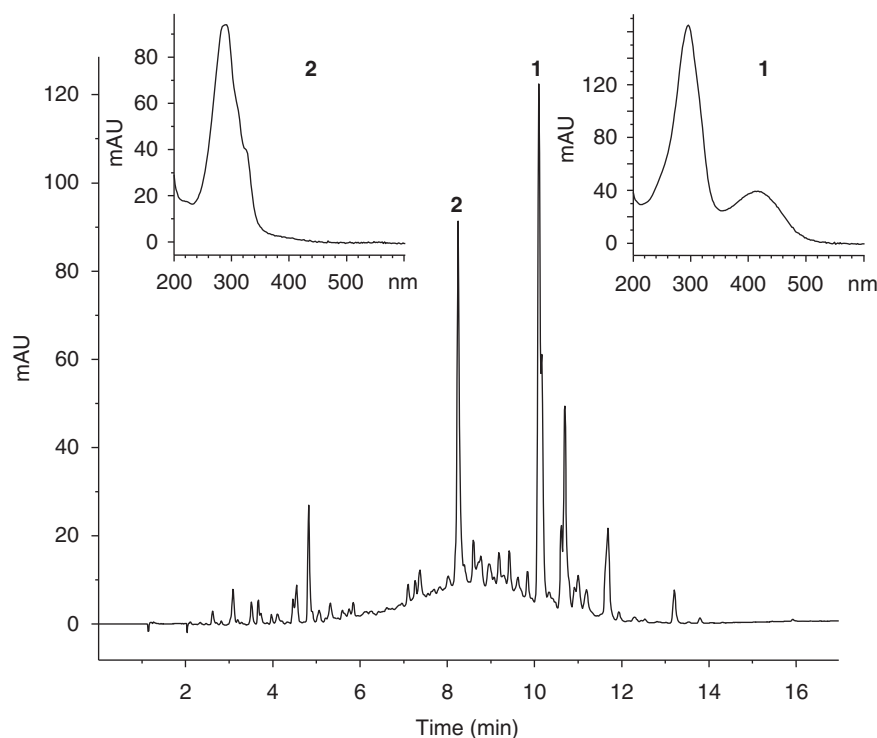


**Figure 2** HPLC analysis of a culture filtrate extract from *Streptomyces* sp. GB 4-2 at a cultivation time of 96 h, monitored at 280 nm; insets: UV-visible spectra of **1** and **2** at retention times of 8.2 min (**2**) and 10.1 min (**1**).

Table 2 NMR assignment of **1** in DMSO-d<sub>6</sub>

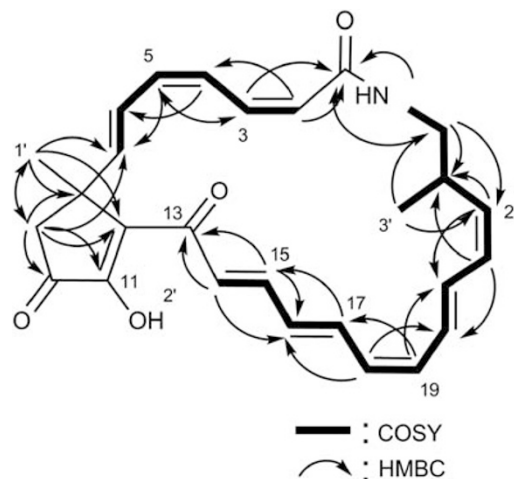
	$\delta$ ( <sup>1</sup> H) [p.p.m.] <i>J</i> in Hz	$\delta$ ( <sup>13</sup> C) [p.p.m.]
1	—	164.4
2	5.08 (d, 11.4)	122.5
3	6.22 (t, 11.8)	132.5
4	7.21 (t, 11.7)	124.2
5	6.10 (dd, 10.1, 14.6)	133.8
6	6.00 (m)	121.3
7	6.00 (m)	143.9
8	—	43.4
9	2.42 (d, 5.53)	49.2
10	—	202.7 <sup>a</sup>
11	—	154.3 <sup>a</sup>
12	—	138.6
13	—	191.8
14	7.24 (m)	129.2
15	7.07 (dd, 11.2, 15.2)	142.4
16	6.56 (dd, 11.1, 14.7)	129.8
17	7.22 (m)	138.5
18	6.20 (t, 10.9)	127.7
19	6.34 (t, 10.2)	134.2
20	6.65 (m)	127.2
21	6.61 (m)	132.2
22	6.06 (t, 9.9)	129.3
23	5.14 (t, 10.2)	136.3
24	2.68 (m)	33.5
25	3.37; 2.65	43.8
26-NH	7.54 (d, 10.2)	—
1'	1.58 (s)	28.6
2'-OH	11.2 (s, br)	—
3'	0.96 (d, 6.34)	17.8

<sup>a</sup>Deduced by HMBC.

methylene carbons, two methyl carbons and one aliphatic quaternary carbon. For compound **2**, the <sup>1</sup>H, <sup>13</sup>C and HSQC NMR data revealed the presence of 23 sp<sup>2</sup>-hybridized carbons, two aliphatic methine carbons, three methylene carbons, three methyl carbons and one aliphatic quaternary carbon. The COSY spectra revealed two spin systems for **1** (H-2–H-7, H-14–H-26–H-3') and three spin systems for **2** (in addition to H-1''–H-3''). By means of HMBC correlations, the systems could be connected through correlations of the amide proton H-26 and C-1. The cyclic pentenone structure could be assigned by the correlations from H-1' to C-7, C-8, C-9, C-12 and the correlations from H-9 to C-1', C-7, C-8, C-10 and C-12. The regiochemistry of the cyclopeptenone was settled by the assignment of <sup>2/3</sup>*J* couplings, particularly from H-1' to the ring carbons C-8, C-9 and C-12. Alternative structural solutions afforded unusual <sup>4</sup>*J* couplings that have not been observed in the other parts of the molecule and therefore have been excluded. In addition, <sup>13</sup>C-NMR chemical shifts are in persuasive accordance to examples from the literature, that is, an α-hydroxy-carbonyl moiety compared with a β-hydroxy-carbonyl moiety.<sup>11,12</sup> By means of COSY and HMBC correlations, the complete carbon chain of **1** could be unambiguously established with the exception of one single correlation connecting C-12 and C-13. Additional HMBC experiments (<sup>4</sup>*J*) with elongated mixing times as well as constant time inverse-detected gradient accordion rescaled-HMBC experiments (*J*=3–12 Hz and *J*=3–8 Hz) for long-range <sup>1</sup>H–<sup>13</sup>C NMR correlations did not yield any conclusive correlations.<sup>13</sup> Hence, this connection was indirectly inferred by the <sup>13</sup>C-chemical shift of C-12 (138.6 p.p.m.), characteristic of an alkene

Table 3 NMR assignment of **2** in DMSO-d<sub>6</sub>

	$\delta$ ( <sup>1</sup> H) [p.p.m.] <i>J</i> in Hz	$\delta$ ( <sup>13</sup> C) [p.p.m.]
1	—	165.8
2	5.57 (d, 10.1)	122.8
3	6.66 (t, 15.6)	131.1
4	6.66 (t, 15.6)	123.3
5	5.86 (t, 11.7)	133.9
6	6.42 (m)	121.8
7	5.64 (d, 15.2)	143.2
8	—	41.3
9	2.33; 2.53 (d, 19.6)	48.1
10	—	204.5 <sup>a</sup>
11	—	156.3 <sup>a</sup>
12	—	138.1
13	—	196.5
14	2.49 (m)	45.5
15	3.48 (dd, 12.1; 14.8)	45.5
16	3.79 (dt, 11.2, 2.96)	43.9
17	5.24 (dd, 10.4; 14.8)	132.7
18	6.35 (dd, 11.4; 14.5)	127.9
19	5.82 (t, 11.1)	127.6
20	5.92 (t, 10.2)	130.1
21	6.44 (m)	127.6
22	6.44 (m)	129.5
23	6.05 (t, 10.5)	129.3
24	5.11 (t, 10.5)	136.3
25	3.09 (m)	31.6
26-NH	2.76 (m)	31.3
1'	3.15 (d, 2.57)	31.3
2'-OH	7.79 (t, 8.84)	—
3'	1.45 (s)	25.0
1''	11.5 (s, br)	—
2''	0.92 (d, 6.48)	17.9
3''	2.74 (m)	31.3
4''-NH	2.63 (dd, 8.57; 13.5)	31.3
5''	4.33 (m)	51.6
6''	—	172.2
1''	8.26 (d, 8.0)	—
2''	—	169.4
3''	1.85 (s)	22.1

<sup>a</sup>Deduced by HMBC.Figure 3 <sup>1</sup>H–<sup>1</sup>H-COSY, HSQC and HMBC correlations observed in **1**.

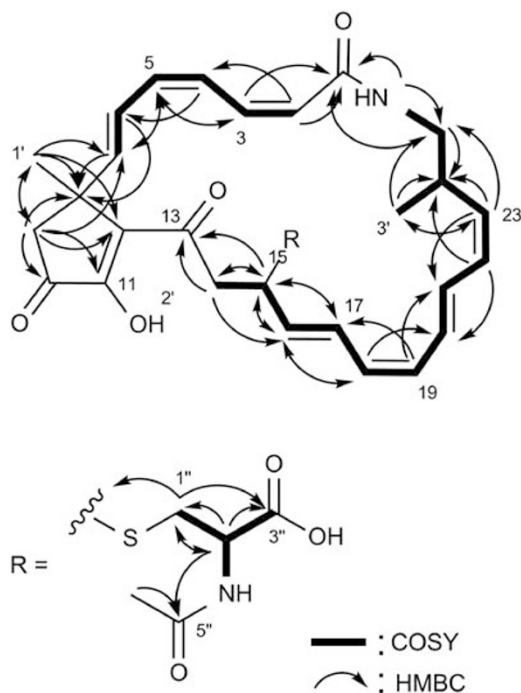


**Figure 4**  $^1\text{H}$ - $^1\text{H}$ -COSY, HSQC and HMBC correlations observed in **2**.

in a vicinal position to carbonyl C-13. Finally, to obtain coupling constants for overlapping proton signals of **1**, selective 1D total correlation spectroscopy experiments were taken from all olefinic protons with mixing time ranging from 70 to 270 ms. These data suggest double bond configurations as shown in Figure 1.

Amino acid analysis of the total acidic hydrolysate of derivative **1** revealed the absence of amino acids in contrast to derivative **2** for which L-cysteine was found. Taking the amino acid analysis and the results from the FT-ICR-MS together, we conclude that **2** is the N-acetyl-L-cysteine adduct of **1**. The linkage to the macrocycle is formed by a thioether to the carbon skeleton, which was further verified by NMR data. The regiochemistry of the N-acetyl-L-cysteine adduct of **2** was deduced from the HMBC experiment, as the  $\beta$ -methylene proton H-1'' of cysteine showed a correlation with C-15 of the polyketide backbone. The addition of N-acetyl-cysteine to C-15 interrupts the large conjugated  $\pi$ -system of **1**, which is supported by a significant alteration of the UV spectrum of **2** compared with **1**.

### Biological activity

**1** showed antibacterial activity against the Gram-positive bacteria, *Bacillus subtilis*, *Staphylococcus aureus*, *S. epidermidis* and *S. lentus* and Gram-negative *Xanthomonas campestris* and also a weak antifungal activity against *Saccharomyces cerevisiae*, *Candida glabrata* and *Botrytis cinerea*. **2** did not show any antimicrobial activity. The minimal inhibitory concentrations of **1** are given in Table 4.

**1** showed a remarkable cytostatic activity against various human tumor cell lines (Table 5), whereas **2** showed no growth inhibitory activity up to a concentration of  $10\ \mu\text{g ml}^{-1}$ .

Enzyme inhibition tests showed an inhibitory activity of **1** against human recombinant protein tyrosine phosphatase 1B (PTP1B) with an  $\text{IC}_{50}$  value of  $10.1\ \mu\text{M}$ . As a reference, the PTP1B inhibitor RK-682 isolated from *Streptomyces* sp.<sup>14</sup> gave an  $\text{IC}_{50}$  value of  $101.1\ \mu\text{M}$  under the same test conditions.

**Table 4** Minimal inhibition concentration of piceamycin (**1**) against Gram-positive bacteria

Organism	MIC [ $\mu\text{g ml}^{-1}$ ]	MIC [ $\mu\text{M}$ ]
<i>Bacillus subtilis</i> DSM 10	0.43	1.00
<i>Bacillus subtilis</i> DSM 347	0.31	0.72
<i>Staphylococcus aureus</i> DSM 20231	0.14	0.33
<i>Staphylococcus lentus</i> DSM 6672	0.45	1.05
<i>Staphylococcus epidermidis</i> DSM 20044	0.11	0.25

**Table 5** Growth inhibitory activity of piceamycin (**1**) ( $\mu\text{g ml}^{-1}$ ) against selected human tumor cell lines

Cell line	$\text{GI}_{50}$	TGI
AGS	0.80	3.4
HepG2	0.30	1.5
MCF 7	0.28	0.7

$\text{GI}_{50}$ : 50% growth inhibition; TGI: 100% growth inhibition.

### DISCUSSION

A comparison of the 23-membered piceamycin (**1**) with other macrocyclic polyketide compounds revealed a structural relationship to hitachimycin, a 19-membered macrolactam antibiotic with anti-protozoal properties isolated from the culture broth of *Streptomyces scabrisporus*.<sup>15</sup> Hitachimycin was found to be identical with the antitumor antibiotic, stubomycin.<sup>16</sup> The structural differences of **1** and hitachimycin are a methyl group at position 8 replacing a hydrogen atom and a methyl group at position 24 replacing a phenyl ring of hitachimycin. Also, the carbonyl group at C-10 in **1** is replaced by a methoxy group in hitachimycin. Similarly, hitachimycin shows antibacterial and cytostatic activities similar to **1**.

The apparent structural difference between **1** and **2** is the N-acetylcysteine moiety covalently attached to the polyketide backbone of **1**. Concomitantly, adduct formation seems to be the reason for the complete absence of the biological activity of adduct **2**. Mechanistically, this finding points to a Michael addition of the nucleophilic thiol group of N-acetylcysteine to C-15 of the Michael system (C-13–C-15) as shown in Figure 4. Other cysteine adducts have not been found thus clearly devising C-15 as the most electrophilic position of **1**. Micro-derivatization experiments monitored by HPLC-MS showed that **1** reacts with L-cysteine to give a molecular mass of a cysteine adduct under standard conditions. According to these data, we suggest that the above-mentioned Michael system is the reason for the antibacterial and cytotoxic effects displayed by **1**.

N-acetylcysteine adducts have been reported earlier, although to our knowledge no adduct with a macrocyclic polyketide has been described. Gilpin *et al.*<sup>17</sup> reported on the antibacterial activity of the phenazine antibiotic, SB 212021, which was completely absent in the N-acetylcysteine derivative, SB 212305.

Besides the remarkable antibacterial and cytostatic activities, **1** also showed high activity against human recombinant protein tyrosine phosphatase 1B ( $\text{IC}_{50}=10\ \mu\text{M}$ ). Small molecule PTP1B inhibitors are of high interest, because of their possible therapeutic application for treatment of diabetes, obesity and cancer.<sup>18</sup>

## EXPERIMENTAL SECTION

### Producing organism and taxonomy

Strain GB 4-2 was isolated from the mycorrhizosphere of a Norway spruce stand in Schönbuch forest near Tübingen (Germany) on a succinate-malate-citrate-humic acid-agar. The strain was examined for morphological and chemotaxonomic properties known to be of value in streptomycete systematics.<sup>8,9</sup>

### Fermentation and isolation

Batch fermentations of strain GB 4-2 were carried out in a 10-l stirred tank fermentor (NB 10; New Brunswick Scientific, Edison, NJ, USA) in a complex medium that consisted of (per liter tap water) oatmeal (Holo Hafergold, Neuform, Germany) 20 g, and trace element solution 5 ml, which was composed of (per liter deionized water) CaCl<sub>2</sub>×2H<sub>2</sub>O 3 g, iron(III) citrate 1 g, MnSO<sub>4</sub>×1H<sub>2</sub>O 200 mg, ZnCl<sub>2</sub> 100 mg, CuSO<sub>4</sub>×5H<sub>2</sub>O 25 mg, Na<sub>2</sub>B<sub>4</sub>O<sub>7</sub>×10H<sub>2</sub>O 20 mg, CoCl<sub>2</sub>×6H<sub>2</sub>O 4 mg and Na<sub>2</sub>MoO<sub>4</sub>×2H<sub>2</sub>O 10 mg; the pH was adjusted to 7.3 (5 M HCl) before sterilization. The fermentor was inoculated with 5% by volume of a shake flask culture grown in a seed medium at 27 °C in 500 ml-Erlenmeyer flasks with a single baffle for 72 h in a rotary shaker at 120 r.p.m. The seed medium consisted of glucose 10 g, glycerol 10 g, oatmeal 5 g, soybean meal (Schoenenberger, Magstadt, Germany) 10 g, yeast extract (Ohly Kat, Deutsche Hefewerke, Hamburg, Germany) 5 g, Bacto casamino acids 5 g and CaCO<sub>3</sub> 1 g in 1 l tap water. The fermentation was carried out for 4 days with an aeration rate of 0.5 volume air/volume/min and agitation at 250 r.p.m.

For isolation of **1**, the fermentation broth was separated by centrifugation into culture filtrate and mycelium. The culture filtrate (8 l) was adjusted to pH 4 (5 M HCl) and extracted three times with EtOAc. The organic extracts were combined and concentrated *in vacuo* to dryness. The crude product was dissolved in CH<sub>2</sub>Cl<sub>2</sub> and added to a diol-modified silica gel column (45×2.6 cm, LiChroprep Diol; Merck, Darmstadt, Germany). The separation was accomplished by a step gradient from CH<sub>2</sub>Cl<sub>2</sub> to 5% MeOH. Fractions containing **1** were combined and concentrated *in vacuo* to a small volume, which was purified by Sephadex LH-20 chromatography (column 90×2.5 cm) in the dark using MeOH as the eluent. To obtain pure **1**, the raw product was subjected to a preparative RP-HPLC column (Reprosil-Pur Basic C18, 10 μm, 25×2.0 cm; Maisch, Ammerbuch, Germany) with MeCN–0.1% HCOOH (52:48) at a flow rate of 20 ml min<sup>-1</sup>.

For isolation of **2**, Hyphlo Super-cel (2%) was added to the fermentation broth, which was separated by multiple sheet filtration into culture filtrate and mycelium. The culture filtrate (8 l) was applied to an Amberlite XAD-16 column (resin volume 800 ml). The resin was washed with 3.2 l H<sub>2</sub>O and H<sub>2</sub>O–MeOH (8:2), and **2** was eluted with 2.4 l H<sub>2</sub>O–MeOH (2:8), concentrated *in vacuo* to an aqueous residue, adjusted to pH 4 and re-extracted three times with EtOAc (each 300 ml). The organic extracts were combined, dissolved in a small volume of MeOH and purified by subsequent chromatography on Sephadex LH-20 and Toyopearl HW-40 (each column 90×2.5 cm) using MeOH as the eluent. To obtain pure **2**, the fractions were separated by preparative RP-HPLC (Nucleosil-100 C-18, 10 μm, 25×1.6 cm; Maisch) with MeCN–0.1% HCOOH using linear gradient elution from 30 to 60% MeCN over 20 min at a flow rate of 20 ml min<sup>-1</sup>.

### HPLC-diode array analyses

The chromatographic system consisted of an HP 1090M liquid chromatograph equipped with a diode-array detector and an HP Kayak XM 600 ChemStation (Agilent Technologies, Waldbronn, Germany). Multiple wavelength monitoring was performed at 210, 230, 260, 280, 310, 360, 435 and 500 nm, and UV-visible spectra were measured from 200 to 600 nm. A 10-ml aliquot of the fermentation broth was centrifuged, and the supernatant was adjusted to pH 4 and extracted with the same volume of EtOAc. After centrifugation, the organic layer was concentrated to dryness *in vacuo* and resuspended in 1 ml MeOH. The corresponding mycelium pellet was extracted with 10 ml MeOH, concentrated to dryness and resuspended in 1 ml MeOH. 10 μl aliquots of the samples were injected onto an HPLC column (125×4.6 mm) fitted with a guard column (20×4.6 mm) filled with 5-μm Nucleosil-100 C-18 (Maisch). The samples were analyzed by linear gradient elution using 0.1% *ortho*-phosphoric acid as solvent

A and MeCN as solvent B at a flow rate of 2 ml min<sup>-1</sup>. The gradient was from 0 to 100% for solvent B in 15 min with a 2-min hold at 100% for solvent B.

### Biological activity

The antimicrobial activity spectrum of **1** and **2** was tested in an agar plate diffusion assay and in a microtiter plate assay against *Bacillus subtilis* DSM 347, *Staphylococcus aureus* DSM 20131, *Escherichia coli* K12, *Xanthomonas campestris* DSM 2405, *Saccharomyces cerevisiae* ATCC 9010, *Candida glabrata* DSM 6425 and *Botrytis cinerea* Tü 157 in a concentration of 0.1–1 mg ml<sup>-1</sup>.

The minimal inhibitory concentration of **1** was tested in a microtiter plate assay using *Bacillus subtilis* DSM 10, *Staphylococcus lentus* DSM 6672, *Staphylococcus epidermidis* DSM 20044 and *Staphylococcus aureus* DSM 20231. The test strains were grown in 96-well microtiter plates with standard concentrations of **1** and incubated for 18–24 h at 27 °C.

The inhibitory activities of **1** and **2** on the growth of tumor cells were tested according to NCI guidelines<sup>19</sup> using human cell lines from gastric adenocarcinoma, breast carcinoma (MCF 7) and hepatocellular carcinoma (HepG2). Cells were grown in 96-well microtiter plates in RPMI-1640 with 10% fetal calf serum in a humidified atmosphere of 5% CO<sub>2</sub> in air. **1** and **2** (0.1–10 μl ml<sup>-1</sup>) were added to the cells after incubation for 24 h. Stock solutions were prepared in DMSO; the final DMSO concentration of the cultures was 0.1%. The cells were fixed and the cell protein analyzed with sulforhodamine B after 48 h incubation.

The inhibitory activity of **1** against human recombinant PTP1B was tested using the Biomol Green PTP1B tyrosine phosphatase drug discovery kit (cat. no. AK822-0001, Biomol, Hamburg, Germany). The PTP1B concentration in the assay was 150 U per well. Optical density was measured at 620 nm using the microtiter plate reader, Infinite M200 (Tecan, Crailsheim, Germany). As a reference for inhibition of PTP1B, RK-682 (cat. no. 557322-200UG, Calbiochem, Darmstadt, Germany) was used.

### Structure elucidation

ESI-MS spectra were obtained on a QTRAP 2000 LC-MS/MS spectrometer (Applied Biosystems, Darmstadt, Germany). High-resolution ESI-FT-ICR mass spectra were recorded on an APEX II FT-ICR mass spectrometer (4.7 T; Bruker-Daltonics, Bremen, Germany), and NMR spectra were recorded on a DRX 500 spectrometer (Bruker, Karlsruhe, Germany) at 500 and 125 MHz for <sup>1</sup>H and <sup>13</sup>C, respectively. The chemical shifts are given in p.p.m. referred to DMSO-*d*<sub>6</sub> as 2.50 p.p.m. (<sup>1</sup>H) and 39.51 (<sup>13</sup>C).

The micro-derivatization experiment was carried out in an HPLC vial with a 20-fold excess of L-cysteine in MeCN at 25 °C and measured after 72 h on a QTRAP 2000 LC-MS/MS spectrometer (Applied Biosystems).

The composition and configuration of the amino acids of **1** and **2** were determined after hydrolysis in 6 M HCl at 110 °C for 24 h. The dry hydrolysate was derivatized to the *N*-(*O*-)TFA/ethyl esters and analyzed by chiral GC-MS on a 20 m×0.25 mm Lipodex E/PS255 (30:70) capillary column.

### ACKNOWLEDGEMENTS

Financial support from the Deutsche Forschungsgemeinschaft (Graduate College 685 'Infection Biology'; DS, JR), the European Commission (project ACTINOGEN, 6th framework, Grant LSHM-CT-2004-005224; RDS), and Bayer Schering Pharma AG (Berlin, Germany) is gratefully acknowledged. We thank Dr Thomas Paululat, Universität Siegen, for helpful discussions and for performing the CIGAR-NMR experiments, and Ms Gaby Biegert, Universität Tübingen, for isolation of streptomycetes strains from rhizospheric soils.

- 1 Hohmann, C. *et al*. Albidopyrone, a new α-pyrone-containing metabolite from marine-derived *Streptomyces* sp. NTK 227. *J. Antibiot.* **62**, 75–79 (2009).
- 2 Garbaye, J. Biological interactions in the mycorrhizosphere. *Experientia* **47**, 370–375 (1991).
- 3 Whipps, J. M. Microbial interactions and biocontrol in the rhizosphere. *J. Exp. Bot.* **52**, 487–511 (2001).
- 4 Tarkka, M. T. & Hampp, R. Secondary metabolites of soil streptomycetes in biotic interactions. In *Secondary Metabolites in Biotic Interactions in Soil* (ed Karlosvski, P.) pp 107–126 (Springer, Berlin, 2008).

- 5 Riedlinger, J. *et al.* Auxofuran, a novel metabolite that stimulates the growth of fly agaric, is produced by the mycorrhiza helper bacterium *Streptomyces* AcH 505. *Appl. Environ. Microbiol.* **72**, 3550–3557 (2006).
- 6 Keller, S., Schneider, K. & Süssmuth, R. D. Structure elucidation of auxofuran, a metabolite involved in stimulating growth of fly agaric, produced by the mycorrhiza helper bacterium *Streptomyces* AcH 505. *J. Antibiot.* **59**, 801–803 (2006).
- 7 Lehr, N.-A., Schrey, S. D., Hampp, R. & Tarkka, M. T. Root inoculation with a forest soil streptomycete leads to locally and systemically increased resistance against phytopathogens in Norway spruce. *New Phytol.* **177**, 965–976 (2008).
- 8 Williams, S. T., Goodfellow, M. & Alderson, G. Genus *Streptomyces* Waksman and Henrici 1943, 339<sup>AL</sup>. In *Bergey's Manual of Systematic Bacteriology* (eds Williams, S.T. *et al*) Vol. 4, pp 2452–3492 (Williams & Wilkins, Baltimore, 1989).
- 9 Manfio, G. P., Zakrzewska-Czerwinska, J., Atalan, E. & Goodfellow, M. Towards minimal standards for the description of *Streptomyces* species. *Biotekhnologiya* **8**, 228–237 (1995).
- 10 Fiedler, H.-P. Biosynthetic capacities of actinomycetes. 1. Screening for novel secondary metabolites by HPLC and UV-visible absorbance spectral libraries. *Nat. Prod. Lett.* **2**, 119–128 (1993).
- 11 Hatsui, T., Nojima, C. & Takeshita, H. Structure elucidation of the pyrolysates formed by 'retro-benzylic acid rearrangement' of the proto-photocycloadducts of methyl 2,4-dioxypentanoate-olefins. *Bull. Chem. Soc. Jpn.* **62**, 2932–2938 (1989).
- 12 Bolvig, S., Duus, F. & Hansen, E. Tautomerism of enolic triacetylmethane, 2-acyl-1,3-cycloalkanediones, 5-acyl-meldrum's acid and 5-acyl-1,3-dimethylbarbituric acids studied by means of deuterium isotope effects on <sup>13</sup>C chemical shifts. *Magn. Reson. Chem.* **36**, 315–324 (1998).
- 13 Hadden, C. E., Martin, G. E. & Krishnamurthy, V. V. Constant time inverse-detection gradient accordion rescaled heteronuclear multiple bond correlation spectroscopy: CIGAR-HMBC. *Magn. Reson. Chem.* **38**, 143–147 (2000).
- 14 Hamaguchi, T., Sudo, T. & Osada, H. RK-682, a potent inhibitor of tyrosine phosphatase, arrested the mammalian cell cycle progression at G1 phase. *FEBS Lett.* **372**, 54–58 (1995).
- 15 Ômura, S., Nakagawa, A., Shibata, K. & Sano, H. The structure of hitachimycin, a novel macrocyclic lactam involving β-phenylalanine. *Tetrahedron Lett.* **23**, 4713–4716 (1982).
- 16 Umezawa, I. *et al.* A new antitumor antibiotic, stubomycin. *J. Antibiot.* **34**, 259–265 (1981).
- 17 Gilpin, M. L., Fulston, M., Payne, D., Cramp, R. & Hood, I. Isolation and structure determination of two novel phenazines from a *Streptomyces* with inhibitory activity against metallo-enzymes, including metallo-β-lactamase. *J. Antibiot.* **48**, 1081–1085 (1995).
- 18 Van Huijsduijnen, R. H., Bombrun, A. & Swinnen, D. Selecting protein tyrosine phosphatases as drug targets. *Drug Discovery Today* **7**, 1013–1019 (2002).
- 19 Grever, M. R., Shepartz, S. A. & Chabner, B. A. The National Cancer Institute: cancer drug discovery and development program. *Semin. Oncol.* **19**, 622–638 (1992).